

# Systematic study of carrier correlations in the electron-hole recombination dynamics of quantum dots

T. Berstermann, T. Auer, H. Kurtze, M. Schwab, D.R. Yakovlev, and M. Bayer  
*Experimentelle Physik II, Universität Dortmund, 44221 Dortmund, Germany*

J. Wiersig, C. Gies, and F. Jahnke  
*Institute for Theoretical Physics, University of Bremen, 28334 Bremen, Germany*

D. Reuter and A.D. Wieck  
*Angewandte Festkörperphysik, Ruhr-Universität Bochum, D-44780 Bochum, Germany*  
(Dated: October 30, 2018)

The ground state carrier dynamics in self-assembled (In,Ga)As/GaAs quantum dots has been studied using time-resolved photoluminescence and transmission. By varying the dot design with respect to confinement and doping, the dynamics is shown to follow in general a non-exponential decay. Only for specific conditions in regard to optical excitation and carrier population, for example, the decay can be well described by a mono-exponential form. For resonant excitation of the ground state transition a strong shortening of the luminescence decay time is observed as compared to the non-resonant case. The results are consistent with a microscopic theory that accounts for deviations from a simple two-level picture.

PACS numbers: 42.25.Kb, 78.55.Cr, 78.67.De

## I. INTRODUCTION

The carrier recombination dynamics in semiconductor quantum dots (QDs) is typically analyzed in terms of exponential decays with a characteristic time constant  $\tau$  in which all possible decay channels are comprised by adding the corresponding decay rates to give the total decay rate  $1/\tau$ . This kind of decay has been adopted from experiments in atomic physics which are discussed using two-level schemes corresponding to the following scenario: An electron has been excited to a higher lying atom shell, from which it relaxes to a vacancy of a lower lying shell. In many cases the relaxation is dominated by radiative recombination, for which mono-exponential decays give an appropriate description of the relaxation process.

Due to the three-dimensional confinement of carriers, semiconductor QDs resemble the solid state analogue of atoms. This has been underlined by the demonstration of effects observed before in atom optics such as a radiatively limited spectral line width [1], antibunching in the single photon emission statistics [2], a square-root power broadening for resonant excitation [3] etc. Most of these results were obtained at cryogenic temperatures. At elevated temperatures the scattering of confined carriers with lattice phonons, for example, becomes strong, as manifested by a strong broadening of the optical transitions [4]. To some extent, this broadening resembles the collision induced broadening of optical transitions in high pressure atom gases.

Furthermore, experiments addressing electron-hole recombination in semiconductors are often performed in a way that not only two electronic levels are involved. Instead, a pulsed laser excites carriers non-resonantly above the barrier, from where they are captured by the confine-

ment potential and relax towards the QD ground state. This situation can be thought to be analogous to a situation in which the atoms have been ionized to a plasma of electrons and ions. During plasma cooling, the electrons are trapped by the ions and relax by photon emission.

Under such conditions the carrier dynamics can in general not be described by a mono-exponential decay, in agreement with many observations reported in literature for QD ensembles. On the other hand, there have been also reports about exponential decays in studies of such ensembles [5]. Also for single QD experiments indications for a non-exponential dynamics have been found [6]. The observed non-exponentiality has been ascribed to various origins such as carrier diffusion to the quantum dots [13, 14], state filling effects due to Pauli blocking [15, 16, 17], inhomogeneities concerning the electron-hole overlap [7, 8, 9, 10, 11, 12], QD potential fluctuations from the quantum confined Stark effect due to charged defects in the QD vicinity [19] as well as formation of optically inactive excitons with parallel electron and hole spins [8, 18]. All these factors may be of relevance for particular experimental situations.

However, many studies have been done for specific situations regarding the QD properties, from which it is hard to develop a systematic picture. Here we have performed time-resolved studies of the carrier dynamics covering a wide range of parameters with respect to these properties such as confinement potential height and residual carrier population. In addition, the optical excitation conditions have been chosen such that many of the factors mentioned above can be ruled out, as described in detail below. For example, the excitation power was chosen so low, that multiexciton effects leading to state filling cannot occur. The influence of carrier diffusion has been ruled out by comparing excitation above the barrier

to excitation below the barrier. By doing so, also the influence of the environment on the confinement potential shape has been under control.

In the following we present a detailed study of the dynamics of carriers in the QD exciton ground state. We show that decays which are to a good approximation mono-exponential can occur, but only under very specific conditions such as fully resonant excitation or very strong QD confinement. Under other circumstances non-exponential decays are found. Interestingly, strictly resonant excitation leads also to a pronounced enhancement of the carrier recombination rate.

The paper is organized as follows. In the next section we briefly discuss the theory of QD photoluminescence [20], which is used to analyze the subsequent experimental studies. In Section III details of the structures under study are given together with a description of the experimental techniques. The experimental data are presented and discussed in Section IV and the comparison with the numerical results is provided in Section V.

## II. THEORY

In our case the dynamics of electrons and holes in QDs was studied by two different spectroscopic techniques: time-resolved photoluminescence and time-resolved transmission. We assume that the carriers quickly loose coherence after their generation by pulsed laser excitation, e.g. by relaxation, so that we address only incoherent electron and hole populations.

(i) The intensity  $I(\omega)$  in time-resolved photoluminescence (TRPL) experiments is given by the temporal evolution of the number of photons from electron-hole recombination at the detection frequency  $\omega$ ,

$$I(\omega) = \frac{d}{dt} \sum_{\xi} \langle b_{\xi}^{\dagger} b_{\xi} \rangle \Big|_{|\mathbf{q}|=\omega/c}, \quad (1)$$

where  $b_{\xi}^{\dagger}$  and  $b_{\xi}$  are the creation and annihilation operators of a photon in state  $\xi$ , which is given by the wave vector  $\mathbf{q}$  and the polarization vector. The brackets  $\langle \dots \rangle$  symbolize the quantum mechanical operator averages.

(ii) A second, independent method, which allows to draw conclusions about the dynamics of the electron and hole populations, is time-resolved differential transmission (TRDT). The electron and hole populations are described by the expectation values  $f_{\nu}^e = \langle e_{\nu}^{\dagger} e_{\nu} \rangle$  and  $f_{\nu}^h = \langle h_{\nu}^{\dagger} h_{\nu} \rangle$ , respectively. Here,  $e_{\nu}^{\dagger}$  and  $e_{\nu}$  ( $h_{\nu}^{\dagger}$  and  $h_{\nu}$ ) are the creation and annihilation operators of an electron (hole) in a state  $\nu$ , including the QD shell index and the spin orientation.

In the following, we are interested in the interplay of photon and population dynamics due to spontaneous re-

combination,

$$\frac{d}{dt} \langle b_{\xi}^{\dagger} b_{\xi} \rangle = \frac{2}{\hbar} \text{Re} \sum_{\nu} g_{\xi\nu}^* \langle b_{\xi}^{\dagger} h_{\nu} e_{\nu} \rangle, \quad (2)$$

$$\frac{d}{dt} f_{\nu}^{(e,h)} \Big|_{\text{opt}} = -\frac{2}{\hbar} \text{Re} \sum_{\xi} g_{\xi\nu}^* \langle b_{\xi}^{\dagger} h_{\nu} e_{\nu} \rangle. \quad (3)$$

The carrier populations are also subject to carrier-carrier Coulomb interaction [26] and to carrier-phonon interaction [27]. The dynamics of both photon and carrier population are determined by the interband photon-assisted polarization  $\langle b_{\xi}^{\dagger} h_{\nu} e_{\nu} \rangle$  and its complex conjugate  $\langle b_{\xi} e_{\nu}^{\dagger} h_{\nu}^{\dagger} \rangle$ . The former describes the emission of a photon due to the recombination of an electron-hole pair, while the latter describes the inverse process, the creation of an electron-hole pair via photon absorption. The strength of the interband polarization is determined by the coupling matrix element of the electron-hole transition to the electromagnetic field,  $g_{\xi\nu}$ .

For solving Eqs. (2) and (3) the interband polarization needs to be known, which is given by its free evolution, by dephasing, by excitonic contributions, by stimulated emission (in the case of QDs embedded into a microcavity [24, 25]), and by spontaneous emission, for which the source term is

$$i \sum_{\alpha} g_{\xi\alpha} \langle e_{\alpha}^{\dagger} e_{\nu} h_{\alpha}^{\dagger} h_{\nu} \rangle. \quad (4)$$

The corresponding equation of motion for this four-particle operator contains averages of six-particle operators, and so on. This is a manifestation of the well-known hierarchy problem of many-particle physics. A consistent truncation scheme is the cluster expansion [28], where all occurring operator expectation values are represented by possible factorizations plus correlations. In our particular case, we use

$$\begin{aligned} \langle e_{\alpha}^{\dagger} e_{\nu} h_{\alpha}^{\dagger} h_{\nu} \rangle &= \langle e_{\alpha}^{\dagger} e_{\nu} \rangle \langle h_{\alpha}^{\dagger} h_{\nu} \rangle \delta_{\alpha\nu} + \delta \langle e_{\alpha}^{\dagger} e_{\nu} h_{\alpha}^{\dagger} h_{\nu} \rangle \\ &= f_{\nu}^e f_{\nu}^h \delta_{\alpha\nu} + C_{\alpha\nu\alpha\nu}^x, \end{aligned} \quad (5)$$

where  $C_{\alpha\nu\alpha\nu}^x = \delta \langle e_{\alpha}^{\dagger} e_{\nu} h_{\alpha}^{\dagger} h_{\nu} \rangle$  is a measure of how strongly the electron-hole pairs are correlated. In the cluster expansion method equations of motion for the correlation contributions are derived. Then the hierarchy of correlation contributions is truncated rather than the hierarchy of expectation values itself. This allows for the consistent inclusion of correlations in the equations of motion up to a certain order in all of the appearing operator expectation values.

For the following analysis, the equations of motion for the carrier populations are further evaluated by assuming a temporally slowly varying interband photon-assisted polarization, so that its adiabatic solution can be used. This leads to [20, 23]

$$\frac{d}{dt} f_{\nu}^{(e,h)} \Big|_{\text{opt}} = -\frac{f_{\nu}^e f_{\nu}^h + \sum_{\alpha} C_{\alpha\nu\alpha\nu}^x}{\tau_{\nu}}, \quad (6)$$

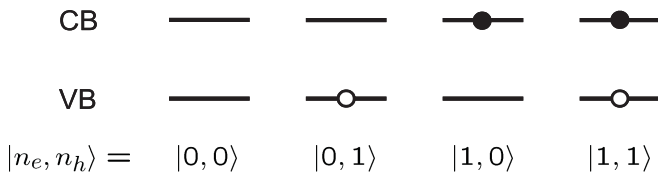


FIG. 1: Possible carrier configurations in the conduction and valence band QD ground states. The spin degree of freedom is neglected.

with the Wigner-Weißkopf decay rate

$$\frac{1}{\tau_\nu} = -\frac{2}{\hbar} \lim_{\Gamma \rightarrow 0^+} \text{Re} \sum_{\xi} \frac{i|g_{\xi\nu}|^2}{\hbar\omega_\nu^e + \hbar\omega_\nu^h - \hbar\omega_\xi - i\Gamma}. \quad (7)$$

In order to illustrate the underlying physics, we consider in the next two paragraphs only s-shell populations and one spin degree of freedom of the carriers. The carrier configuration can then be expanded into the basis set  $|n_e, n_h\rangle$ , where the  $n_e$  and  $n_h$  give the number of electrons and holes, respectively (the photonic part of the states is of no relevance here and not shown). The possible configurations are  $|0,0\rangle$ ,  $|0,1\rangle$ ,  $|1,0\rangle$  and  $|1,1\rangle$ , as displayed schematically in Figure 1.

If the electron and hole populations were fully correlated, only  $|0,0\rangle$  and  $|1,1\rangle$  out of these 4 configurations would be relevant. Using the following relations for the electron and hole number operators  $e^\dagger e|0,0\rangle = h^\dagger h|0,0\rangle = 0$  and  $e^\dagger e|1,1\rangle = h^\dagger h|1,1\rangle = |1,1\rangle$  we see that in this *two-level case*  $\langle e^\dagger e h^\dagger h \rangle$  reduces to  $f^e = \langle e^\dagger e \rangle$  and also  $f^h = \langle h^\dagger h \rangle$ . In this particular situation, the source term of spontaneous emission  $f^e f^h + C^x = \langle e^\dagger e h^\dagger h \rangle$  in Eq. (6) can be replaced by  $f^{(e,h)}$ , and then the equations of motion give a single-exponential decay. As soon as the other two configurations are included, Eq. (6) in general results in a non-exponential decay. In Section V we evaluate  $C^x$  under more general conditions.

### III. SAMPLES AND EXPERIMENT

The experiments were performed on different types of self-assembled (In,Ga)As/GaAs QD arrays fabricated by molecular beam epitaxy. All samples contained 20 layers of QDs, which were separated from one another by 60-nm-wide barriers. The first type of QDs was nominally undoped, the other two types were modulation doped, one of n-type and the other one of p-type. The Silicon- or Carbon-doping layers were located 20 nm below each dot layer. The dopant density was chosen about equal to the dot density in each layer, so that an average occupation by a single electron or hole per dot can be expected.

The photoluminescence emissions of the as-grown QD samples are located around 1200 nm at cryogenic temperatures for all three dot types. In order to vary the confinement potential, several pieces from each QD sample type were thermally annealed for 30 s at different temperatures  $T_{ann}$  between 800 and 980 °C. Because of the

annealing the confinement is reduced due to intermixing of dot and barrier material. Typical photoluminescence spectra of the nominally undoped samples, which show the established behavior for such a series of annealed QD structures can be found in Ref. [29]. Increasing  $T_{ann}$  results in a blueshift as well as a narrowing of the emission line from the ground state exciton. The corresponding blue shift of the wetting layer is found to be rather weak as compared to that of the QD emission. Therefore the confinement potential, which we define as the energy separation between the wetting layer emission and the QD ground state emission, varies systematically within an annealing series. The confinement energies increase from about 50 up to 400 meV with decreasing  $T_{ann}$ .

The QD samples were mounted on the cold finger of a microscopy flow-cryostat which allows for temperature variations down to 6K. In the TRPL studies a mode-locked Ti-sapphire laser emitting linearly polarized pulses with a duration of about 1 ps at 75.6 MHz repetition rate (corresponding to 13.2 ns pulse separation) was used for optical excitation. The QD luminescence was dispersed by a monochromator with 0.5 m focal length and detected by a streak camera with a S1 photocathode. In the standard synchroscan configuration, time ranges up to 2 ns could be scanned with a resolution of about 20 ps. Longer time ranges could be addressed by installing a long delay time unit of about 50 ps. The excitation was kept as weak as possible to avoid multiexciton effects.

In the TRDT studies two synchronized Ti-sapphire lasers with a jitter well below 1 ps were used for the excitation. The emission energies could be varied independently. One laser beam, the pump, was used for the creation of carrier populations while the other one, the probe, was used to test them. The temporal delay between both pulses could be varied by a mechanical delay line, along which the probe beam was sent. The transmission of the probe was detected with a homodyne technique based on phase-sensitive balanced detection. The polarization of the pump and the probe beam were chosen either linear or circular co-polarized.

We mention already here that the main topic of our studies is not the quantitative values of the decay times, which have been addressed already in many other studies. The focus is instead to develop a systematic picture of the dependence of the recombination on experimental parameters, both the internal QD properties and the external conditions such as excitation energy and intensity.

### IV. RESULTS AND DISCUSSION

The outline of the carrier recombination dynamics in Section II provides a guide for the experimental studies. An exponential decay could occur if the carrier populations were correlated, i.e., excitonic correlations were present. However, in experiments, in which the carriers are created by non-resonant excitation into the wetting layer or the barrier, electrons and holes typically relax

independently towards their QD ground states. In this evolution of the carrier population, dephasing due to carrier scattering competes with the necessary built-up of excitonic correlations. It has been discussed for quantum wells in [30] that the formation process might take longer than the recombination process. For QDs it has been shown in [20] that, while electrons and holes are still localized by the strong confinement potential, excitonic correlations are easily suppressed by dephasing processes related to carrier scattering.

In general, the analysis leading to Eq. (6) has shown that the recombination dynamics is determined by (i) the electron and hole populations, and (ii) the Coulomb correlations between the carriers. The high flexibility in fabricating self-assembled QDs allows us to tailor the corresponding parameters such that their impact can be systematically tested. In detail, the following experiments have been performed:

(i) The electron and hole populations have been varied by studying the carrier dynamics in undoped QDs in comparison to those in either n-type or p-type doped QDs.

(ii) Coulomb interaction can lead to carrier scattering between QD shells. The carrier scattering can be enhanced by reducing the shell splitting. Therefore the influence of correlations has been studied by addressing dots with different confinement heights.

(iii) The correlations can affect carrier scattering only if enough excess energy is available to fulfil energy conservation in the scattering event. This excess energy can be varied by the photon energy of the exciting laser.

### A. Influence of excitation energy

First we discuss the influence of the available excess energy on the exciton recombination dynamics. For that purpose, the excitation was decreased from being non-resonant into the GaAs barrier to being into the wetting layer, and further into the confined QD states. Figure 2 shows transients of the electron-hole recombination from the ground state of nominally undoped (In,Ga)As/GaAs QDs with a confinement potential of about 80 meV, i.e. the confinement potential in these dots is rather shallow. The excitation pulse hit the sample at time zero. Note the logarithmic scale on the left scale.

The top trace shows the result for the GaAs excitation. After a typical rise of the signal during a few tens of ps, the intensity drops on a few hundred ps time scale. The solid line shows an attempt to fit a mono-exponential decay to the data at early times. For the fit the first 300 ps after the PL plateau maximum have been used, in this case from 200 to 500 ps. After about a nanosecond, a clear deviation from this decay can be seen, as expected from our theoretical model. This deviation becomes more pronounced for wetting layer excitation, for which already after 700 ps the non-exponential behavior of the decay becomes obvious. Note further that the rise

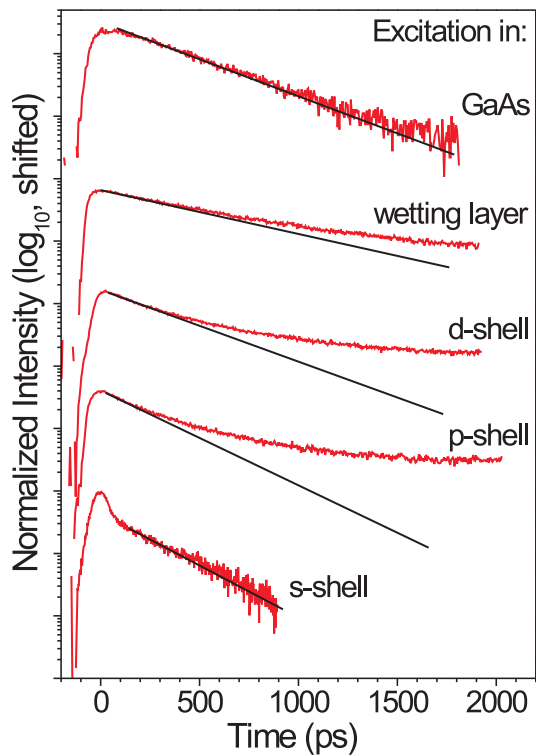


FIG. 2: TRPL transients of undoped (In,Ga)As/GaAs self-assembled QDs with a confinement potential height of 80 meV. Pulsed excitation occurred at time zero. Detected was the ground state luminescence. The energy position of the exciting laser is indicated at each trace. The lines are attempts to fit the data in a time range of 300 ps after the transient starts to show a clear decay. For resonant excitation the signal is influenced by scattered laser light around time zero.  $T = 10$  K. The energy of the exciting laser for GaAs, wetting layer, d-shell, p-shell, s-shell has been set to 1.550 eV, 1.476 eV, 1.436 eV, 1.414 eV, 1.389 eV respectively. The average excitation density was  $0.7 \text{ kW/cm}^2$ .

time of the signal is reduced as compared to the case of GaAs excitation.

The non-exponential decay is also seen if the excitation is done below the barrier into the d-shell or the p-shell of the QDs, as demonstrated by the two mid traces. It has become even more pronounced than for above barrier illumination, as the deviation becomes apparent already at earlier delays below 500 ps. At these delays the decay appears to be faster which might be related to a more rapid relaxation into the ground state.

Note that these results for below barrier excitation also show that the deviation from exponentiality cannot be traced to dark excitons, whose radiative decay requires a spin-flip first. As soon as carriers are trapped in the QDs, spin relaxation is strongly suppressed at low  $T$ , in particular because the spin-orbit coupling mechanisms which are very efficient in higher dimensional systems are strongly suppressed. [21, 22]. The resulting flip times are in the microseconds range and may even reach milliseconds, which is by far too long to give any significant con-

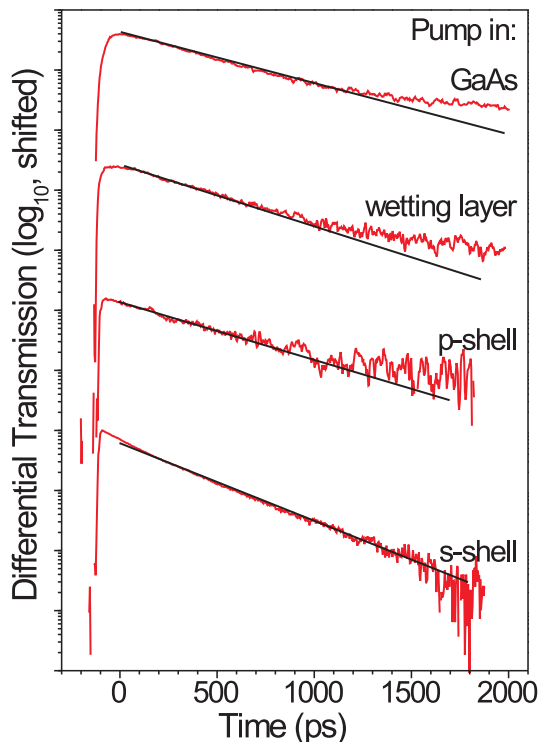


FIG. 3: TRDT transients of the (In,Ga)As/GaAs self-assembled QDs with a confinement potential height of 80 meV studied also in Fig. 2. The ground state populations were probed for different excitation energies of the pump laser as indicated at each trace. The lines are linear fits to the data in the time range from 200 to 500 ps.  $T = 10$  K. The energies of the pump laser for GaAs, wetting layer, d-shell, p-shell, s-shell were the same as in the TRPL experiments. The average pump (probe) density was  $0.07$  kW/cm<sup>2</sup> ( $0.007$  kW/cm<sup>2</sup>).

tribution to the decay dynamics in the monitored time range.

This is consistent with previous observation that the exciton spin-flip time exceeds tens of ns [31]. In the experiment here with a 75.6 MHz laser repetition rate a dark exciton contribution would appear as constant background at the low temperatures applied. This is confirmed in studies where the laser repetition rate was reduced: A slowly decaying background appears in these experiments for delays exceeding 10 ns, at which all recombination processes involving optically active excitons took place.

Varying the excitation power in the regime where multiexciton effects are negligible leads also to slight variations of the decay dynamics: For non-resonant excitation the decay tends to be slowed down in the range of 10%, while for excitation into higher lying QD states the changes are weak. For non-resonant excitation, the deceleration might be attributed to enhanced carrier diffusion before carrier trapping can occur. For carrier-carrier scattering which additionally supports the phonon-assisted relaxation. These observations generally complicate the interpretation of decay times determined

under non-resonant conditions as exciton lifetimes and, in particular, the comparison for different samples, as long as the change does not lie outside of the observed variation range.

The bottom trace of Fig. 2, finally, shows the TRPL for resonant excitation between the valence and conduction band ground states. Around zero delay scattered light from the laser is seen. After  $\sim 50$  ps a decay becomes prominent, which is within the experimental accuracy purely exponential, in contrast to the previous non-resonant excitation conditions. Furthermore, the decay is much faster than before. Comparing the decay time to those determined by fitting the early delay data under non-resonant conditions, we find an acceleration by a factor of about 2. For non-resonant excitation the optically excited polarization is converted into populations by the scattering involved in the relaxation. For resonant excitation, on the other hand, the carrier coherence is maintained until recombination occurs, as recent four-wave-mixing studies have demonstrated [1]. Therefore under these conditions coherent luminescence is observed. Corresponding calculations are very involved as they require additional inclusion of interband coherence terms in the dynamics. However, from the theory in the incoherent regime we expect strong carrier correlations in the case of resonant excitation, i.e. for the source term of spontaneous emission we have  $f^e f^h + C^x \approx f^e$ . Hence, since  $f^e > f^e f^h$ , Eq. (6) predicts a faster decay for resonant excitation.

The TRPL results are confirmed by TRDT studies shown in Fig. 3. The energy of the pump beam was tuned in the same way as in the TRPL studies described above. The energy of the probe was fixed to the s-shell. The shape of the different traces is very similar to those observed in TRPL. For excitation into GaAs the transmission clearly deviates from an exponential decay, and the same is true for excitation into the wetting layer, the d-shell (not shown, very similar to the p-shell case) and the p-shell. In contrast, for resonant excitation an exponential decay is observed again with a characteristic time significantly shorter than that for non-resonant excitation.

Under these conditions the exponential decay constants are 310 ps for the TRDT experiment and 280 ps in the case of the TRPL measurement.

## B. Influence of doping

Neglecting the influence of Coulomb correlations, according to Eq. (6) the carrier population dynamics can be pushed towards a mono-exponential decay if either the electron or the hole population is approximately held constant. This can be achieved by a background doping, for which we studied both n- and p-doped samples which were prepared such that there is on average a single carrier per dot. The studies show that besides variations in the quantitative values for the decay times the shape is

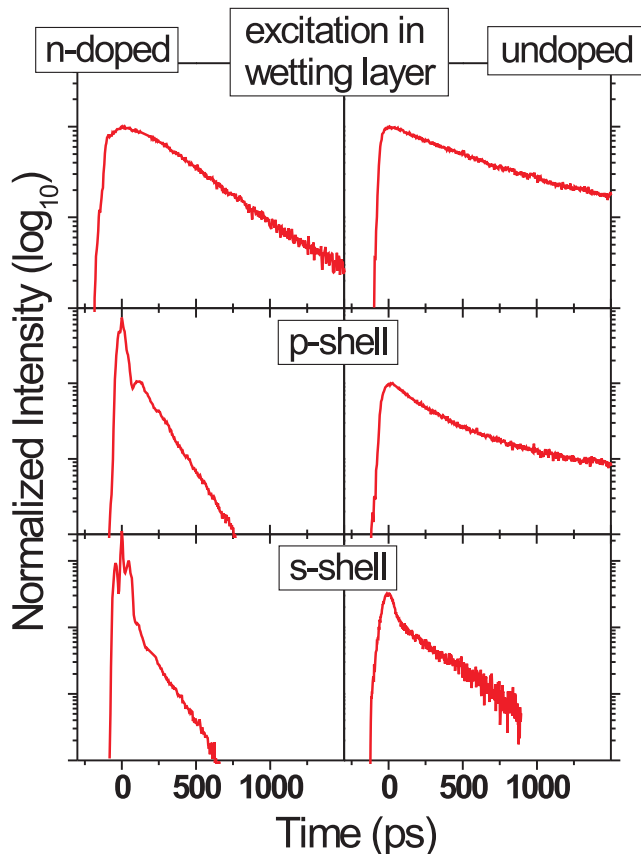


FIG. 4: Comparison of TRPL traces for n-doped (left panels) and undoped (right panels) QDs excited at different energies, as labelled in each figure. The height of the confinement potential is about 80 meV. Around time zero the signal is influenced by scattered laser light.  $T = 10$  K. The excitation energy for the n-doped sample in GaAs, wetting layer, d-shell, p-shell, s-shell has been set to 1.550 eV, 1.476 eV, 1.437 eV, 1.417 eV, 1.397 eV respectively. The average excitation density was 0.7 kW/cm<sup>2</sup>.

very similar, independent of the type of doping. Therefore we focus on the n-doped structures only.

Figure 4 depicts the corresponding TRPL results for n-doped QDs, excited at different energies. The confinement potential was about 80 meV. For comparison the data for the undoped dots from Fig. 2 are also shown. Clearly, the decay behavior of the doped dots comes much closer to an exponential decay, independent of the actual excitation energy. Again, only for resonant excitation, however, mono-exponential decays are seen in both cases.

For non-resonant excitation such as in GaAs also the n-doped QDs show a deviation from an exponential decay at long delays. While this might be well correlated with the influence of correlation induced scattering, we cannot exclude some contribution from charge neutral QDs, where the charge depletion might partly arise from above barrier photoexcitation.

We note that these results give also some hint why the PL decay in the undoped QDs is closer to an exponential

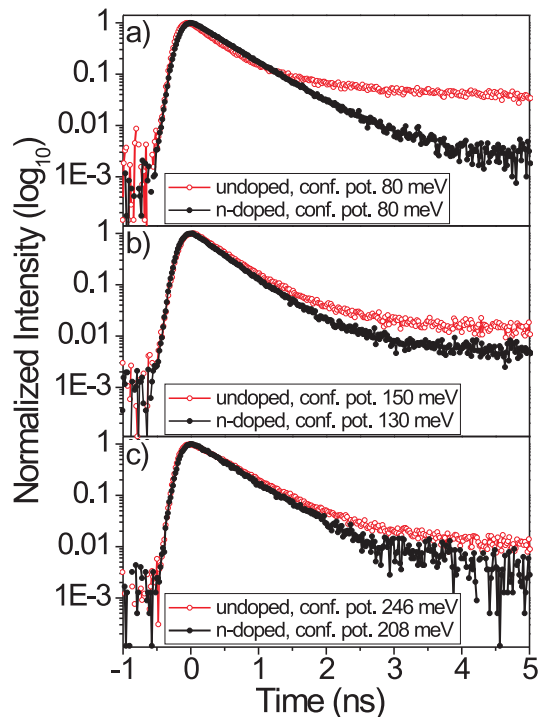


FIG. 5: TRPL transients for undoped (open symbols) and n-doped (full symbols) QDs with different confinement potentials, as indicated in each panel. Excitation was done into GaAs at 1.550 eV.  $T = 10$  K, excitation density 0.7 kW/cm<sup>2</sup>.

behavior for excitation into GaAs than for wetting layer excitation. It is well known that non-resonant excitation into the barrier may lead to a formation of charged excitons, for which the decay in Fig. 4 is almost exponential. Formation of charged complexes is strongly suppressed for below barrier excitation in undoped QDs.

### C. Influence of correlations

The magnitude of the correlations between carriers due to Coulomb interaction can be tailored by varying the QD confinement. With increasing confinement potential the splitting between the dot shells increases, while possible scattering (that suppresses correlations) is reduced. This was studied by comparing QDs annealed at different temperatures. Figure 5 shows the results for QD samples which were excited non-resonantly into GaAs. For comparison, again the data for undoped and n-doped QDs are displayed. The height of the confinement potentials increased from 80 (80) to 150 (130) and further to 250 (210) meV for undoped (n-doped) structures. The resulting splittings between the confined QD shells, as estimated from high excitation PL spectroscopy, are 20, 35, and 50 meV, respectively.

In all cases it can be seen that the dynamics in the undoped dots deviates more strongly from an exponential decay than that in the doped structures. However, with

increasing confinement the difference becomes smaller, and for the strongest confinement the traces almost coincide. In this particular case the influence of the Coulomb scattering has been reduced to an extent that it is no longer relevant for the dephasing of correlations.

## V. NUMERICAL RESULTS

In this section we provide exemplary numerical results which support the previous conclusions. The semiconductor luminescence equations (SLE) are used to describe the time evolution of the photon number  $\langle b_\xi^\dagger b_\xi \rangle$ , the carrier populations  $f_\nu^{(e,h)}$ , the photon-assisted polarization  $\langle b_\xi^\dagger h_\nu e_\nu \rangle$ , and the carrier-carrier correlations such as  $C_{\alpha\nu\alpha\nu}^x = \delta \langle e_\alpha^\dagger e_\nu h_\alpha^\dagger h_\nu \rangle$ . Scattering is treated in relaxation-time approximation. We restrict ourselves to the formulation of the theory in the incoherent regime, as presented in [20], and consider nonresonant excitation. The QD parameters are those used in Ref. [20], except the QD density is  $N = 10^{10} \text{ cm}^{-2}$ , the dipole moment is  $16.8e\text{\AA}$  and the dephasing of the correlations is  $0.05 \text{ meV}$ . Even though the dephasing is weak it effectively destroys the correlations on a time scale of tens of ps.

Figure 6 shows results for undoped and n-doped QDs excited in the p-shell. For the undoped situation we pump the system with equal electron and hole density  $N_e = N_h = 0.35N$ . In the n-doped case we assume on average one additional electron per QD, i.e.  $N_e = N_h + N$  with again  $N_h = 0.35N$ . Apart from this difference in the initial conditions both curves have been calculated with exactly the same parameters. An agreement between theory and experiment can be observed: (i) the doped QDs show an exponential decay, whereas the undoped ones show a non-exponential decay. (ii) the decay is much faster for the doped QDs if compared to the undoped QDs.

To understand the origin of these different behaviors, it is illuminating to study the time evolution of the s-shell populations as depicted in Fig. 7 for one spin subsystem. In the undoped case the s-shell populations are zero at first. Due to the pump process and the subsequent carrier scattering, the s-shell population increases temporarily and decays subsequently to its initial value. In the n-doped case the electron occupation in the s-shell starts with the finite value of 0.5 due to the doping. The temporal change of the electron population relative to the doping level is small. According to Eq. (6), a constant electron population  $f_\alpha^e$  leads to an exponential decay of the hole population  $f_\alpha^h$  and, hence, of the PL-intensity for the considered situation of strong suppression of excitonic correlations  $C^x$  due to dephasing.

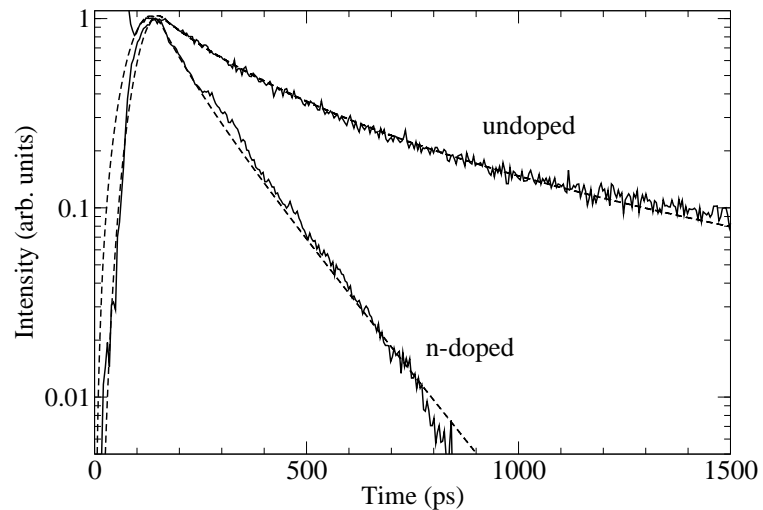


FIG. 6: Calculated TRPL intensity (dashed lines) according to Eq. (1) for pumping into the p-shell of undoped and n-doped QDs. The experimental data (solid lines) are the same as in Fig. 4.

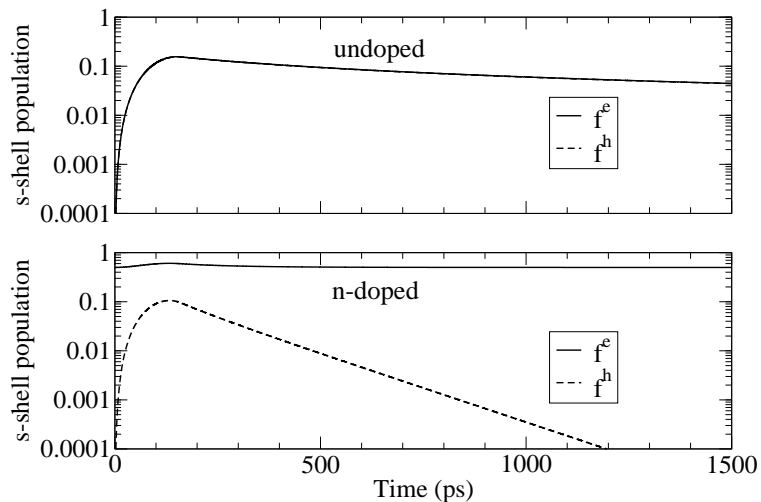


FIG. 7: Time evolution of electron and hole populations,  $f^e$  and  $f^h$  in the s-shell of undoped (top) and n-doped (bottom) QDs. The population is defined such that it is unity if the s-shell is populated by two carriers with opposite spin. Single carrier population corresponds to a 0.5 population accordingly.

## VI. CONCLUSIONS

In summary, we have performed a detailed study of the carrier recombination dynamics in QDs. The results show that the carrier recombination in general follows a non-exponential decay. Only under specific conditions, like resonant excitation, strong confinement, or intentional doping, a mono-exponential decay is observed. In addition, ensuring coherence of the excited carriers by resonant excitation leads to a strong shortening of the decay time. The experimental results are in excellent

agreement with numerical results obtained from a microscopic theory which abandons the shortcomings of the commonly used two-level description of QDs.

**Acknowledgements.** We gratefully acknowledge the financial support of this work by the Deutsche

Forschungsgemeinschaft (research group ‘Quantum Optics in Semiconductor Nanostructures’ and the research project BA 1549/10-1). The Bremen group acknowledges a grant for CPU time at the NIC, Forschungszentrum Jülich.

- 
- [1] W. Langbein, P. Borri, U. Woggon, V. Stavarache, D. Reuter, and A. D. Wieck, *Phys. Rev. B* **70**, 033301 (2004).
- [2] P. Michler, A. Imamoglu, M. D. Mason, P. J. Carson, G. F. Strouse and S. K. Buratto, *Nature* **406**, 968 (2000).
- [3] A. Stuffer, P. Ester, A. Zrenner, and M. Bichler, *Phys. Rev. B* **72**, 121301 (2005).
- [4] see, for example, P. Borri, W. Langbein, S. Schneider, and U. Woggon, R. L. Sellin, D. Ouyang, and D. Bimberg, *Phys. Rev. Lett.* **87**, 157401 (2001); M. Bayer and A. Forchel, *Phys. Rev. B* **65**, 041308 (2002).
- [5] see, for example, W. Yang, R.-R. Lowe-Webb, H. Lee, and P.C. Sercel, *Phys. Rev. B* **56**, 13314 (2005); S. Raymond, S. Fafard, P. J. Poole, A. Wojs, P. Hawrylak, S. Charbonneau, D. Leonard, R. Leon, P. M. Petroff, and J. L. Merz, *Phys. Rev. B* **54**, 13314 (2005); F. Adler, M. Geiger, A. Bauknecht, D. Haase, P. Ernst, A. Dörnen, F. Scholz, H. Schweizer, *J. Appl. Phys.* **83**, 1631 (1998).
- [6] J. Hours, P. Senellart, E. Peter, A. Cavanna, and J. Bloch *Phys. Rev. B* **71**, 161306 (2005)
- [7] R. A. Oliver, G. Andrew, D. Briggs, M. J. Kappers, C. J. Humphreys, J.H. Rice, J. D. Smith, and R. A. Taylor, *Appl. Phys. Lett.* **83**, 755 (2003).
- [8] O. Labeau, P. Tamarat, and B. Lounis, *Phys. Rev. Lett.* **90**, 257404 (2003).
- [9] I. L. Krestnikov, N. N. Ledentsov, A. Hoffmann, D. Bimberg, A. V. Sakharov, W. V. Lundin, A. F. Tsatsul’nikov, A. S. Usikov, Zh. I. Alferov, Yu. G. Musikhin, and D. Gerthsen, *Phys. Rev. B* **66**, 155310 (2002).
- [10] B. V. Kamenev, J.-M. Baribeau, D. J. Lockwood, and L. Tsybeskov, *Physica E* **26**, 174 (2005).
- [11] A. S. Dissanayake, J. Y. Lin, and H. X. Jiang, *Phys. Rev. B* **51**, 5457 (1995).
- [12] Yu-Shen Yuang, Yang-Fang Chen, Yang-Yao Lee, and Li-Chi Liu, *J. Appl. Phys.* **76**, 3041 (1994).
- [13] F. Adler, M. Geiger, A. Bauknecht, D. Haase, P. Ernst, A. Dörnen, F. Scholz, and H. Schweizer, *J. Appl. Phys.* **83**, 1631 (1998).
- [14] A. Melliti, M. A. Maaref, F. Hassen, M. Hjiri, H. Maaref, J. Tignon, and B. Sermage, *Sol. State Commun.* **128**, 213 (2003).
- [15] V. Zwiller, M. E. Pistol, D. Hessmann, R. Cederström, W. Seifert, and L. Samuelson, *Phys. Rev. B* **59**, 5021 (1999).
- [16] F. Adler, M. Geiger, A. Bauknecht, F. Scholz, H. Schweizer, M. H. Pilkuhn, B. Ohnesorge, and A. Forchel, *J. Appl. Phys.* **80**, 4019 (1996).
- [17] S. Raymond, S. Fafard, P. J. Poole, A. Wojs, P. Hawrylak, S. Charbonneau, D. Leonard, R. Leon, P. M. Petroff, and J. L. Merz, *Phys. Rev. B* **54**, 11548 (1996).
- [18] B. Patton, W. Langbein, and U. Woggon, *Phys. Rev. B* **68**, 125316 (2003).
- [19] V. Türck, S. Rodt, O. Stier, R. Heitz, R. Engelhardt, U. W. Pohl, and D. Bimberg, *Phys. Rev. B* **61**, 9944 (2000).
- [20] N. Baer, C. Gies, J. Wiersig, and F. Jahnke, *Eur. Phys. J. B* **50**, 411 (2006).
- [21] A. V. Khaetskii, D. Loss, and L. Glatzman, *Phys. Rev. Lett.* **88**, 186802 (2002); I. A. Merkulov, Al. L. Efros, and M. Rosen, *Phys. Rev. B* **65**, 205309 (2002); R. de Sousa, and S. Das Sarma, *ibid.* **67**, 033301 (2003); L. M. Woods, T.L. Reinecke, and Y. Lyanda-Geller, *ibid.* **66**, 161318 (2002); L. M. Woods, T. L. Reinecke, and R. Kotlyar, *ibid.* **69**, 125330 (2004).
- [22] T. Brandes, and T. Vorrath, *Phys. Rev. B* **66**, 075341 (2002); V. N. Golovach, A. Khaetskii, and D. Loss, *Phys. Rev. Lett.* **94**, 016601 (2002); R. Hanson, B. Witkamp, L. M. K. Vandersypen, L. H. Willems van Beveren, J. M. Elzerman, and L. P. Kouwenhoven, *ibid.* **91**, 196802 (2003).
- [23] M. Schwab, H. Kurtze, T. Auer, T. Berstermann, M. Bayer, J. Wiersig, N. Baer, C. Gies, F. Jahnke, J.P. Reithmaier, A. Forchel, M. Benyoucef, and P. Michler, *Phys. Rev. B* **74**, 045323 (2006).
- [24] C. Gies, J. Wiersig, M. Lorke, and F. Jahnke, *Phys. Rev. A* **75**, 013803 (2007).
- [25] S. M. Ulrich, C. Gies, S. Ates, J. Wiersig, S. Reitzenstein, C. Hofmann, A. Löffler, A. Forchel, F. Jahnke, and P. Michler, *Phys. Rev. Lett.* **98**, 043906 (2007).
- [26] T. R. Nielsen, P. Gartner, and F. Jahnke, *Phys. Rev. B* **69**, 235314 (2004).
- [27] J. Seebeck, T. R. Nielsen, P. Gartner, and F. Jahnke, *Phys. Rev. B* **71**, 125327 (2005).
- [28] J. Fricke, *Ann. Phys.* **252**, 479 (1996).
- [29] A. Greilich, M. Schwab, T. Berstermann, T. Auer, R. Oulton, D. R. Yakovlev, and M. Bayer, *Phys. Rev. B* **73**, 045323 (2006).
- [30] W. Hoyer, M. Kira, and S. W. Koch, *Phys. Rev. B* **67**, 155113 (2003).
- [31] M. Paillard, X. Marie, P. Renucci, T. Amand, A. Jbeli, and J. M. Gérard, *Phys. Rev. Lett.* **86**, 1634 (2001).